



Universidad Autónoma
de Madrid

Biblos-e Archivo
Repositorio Institucional UAM

Repositorio Institucional de la Universidad Autónoma de Madrid
<https://repositorio.uam.es>

Esta es la **versión de autor** del artículo publicado en:
This is an **author produced version** of a paper published in:

Clinical Cancer Research 23.20 (2017): 6315-6325

DOI: <https://doi.org/10.1158/1078-0432.CCR-16-2250>

Copyright: © 2017 American Association for Cancer Research

El acceso a la versión del editor puede requerir la suscripción del recurso
Access to the published version may require subscription

TITLE: Targeted exome sequencing of Krebs cycle genes reveals candidate cancer predisposing mutations in pheochromocytomas and paragangliomas

Laura Remacha^{1†}, Iñaki Comino-Méndez^{1†}, Susan Richter², Laura Contreras^{3,4}, María Currás-Freixes¹, Guillermo Pita⁵, Rocío Letón¹, Antonio Galarreta¹, Rafael Torres-Pérez¹, Emiliano Honrado⁶, Scherezade Jiménez⁷, Lorena Maestre⁷, Sebastian Moran⁸, Manel Esteller⁸, Jorgina Satrústegui^{3,4}, Graeme Eisenhofer², Mercedes Robledo^{1,3}, and Alberto Cascón^{1,3}

¹Hereditary Endocrine Cancer Group, Spanish National Cancer Research Centre (CNIO), Madrid, Spain

²Institute of Clinical Chemistry and Laboratory Medicine, University Hospital Carl Gustav Carus, Medical Faculty Carl Gustav Carus, Technische Universität Dresden, Dresden, Germany

³Centro de Investigación Biomédica en Red de Enfermedades Raras (CIBERER), Madrid, Spain

⁴Departamento de Biología Molecular, Centro de Biología Molecular Severo Ochoa UAM-CSIC, Universidad Autónoma de Madrid and Instituto de Investigación Sanitaria Fundación Jiménez Díaz (IIS-FJD), Madrid, Spain

⁵Human Genotyping Unit-CeGen, Human Cancer Genetics Programme, Spanish National Cancer Research Centre (CNIO), Madrid, Spain

⁶Anatomical Pathology Service, Hospital de León, León, Spain

⁷Monoclonal Antibodies Unit, Biotechnology Programme, Spanish National Cancer Research Centre (CNIO), Madrid, Spain

⁸Cancer Epigenetics and Biology Program (PEBC), Bellvitge Biomedical Research Institute (IDIBELL), L'Hospitalet, Barcelona, Spain.

[†]These two authors contributed equally to this article.

RUNNING TITLE: Novel mutations in TCA genes in pheochromocytoma/paraganglioma

Keywords: Krebs cycle, *GOT2*, pheochromocytoma, paraganglioma, targeted exome sequencing.

Grant Support

This work was supported by the *Fondo de Investigaciones Sanitarias* project PI15/00783 to A.C and the Deutsche Forschungsgemeinschaft (grant RI 2684/1-1) to S.R. CEGEN-PRB2-ISCI is supported by grant PT13/0001, ISCI-SGEFI/FEDER.

Corresponding author: Alberto Cascón, Hereditary Endocrine Cancer Group, Human Cancer Genetics Programme, Spanish National Cancer Research Centre (CNIO), Melchor Fernández Almagro 3, 28029 Madrid, Spain. Phone: +34 91 224 69 47. Fax: +34 91 224 69 23. E-mail: acascon@cnio.es

Translational Relevance

Mutations in pheochromocytoma (PCC)/paraganglioma (PGL) predisposition genes encoding enzymes involved in the Krebs cycle lead to a particular CpG island hypermethylation phenotype in these tumors. We used selected tumors with this phenotype for targeted exome sequencing of a panel of Krebs cycle-related genes in order to find new PCC/PGL susceptibility genes. Apart from known cancer-predisposing somatic alterations in *IDH1* and *SDHC*, we found a germline variant in *GOT2*. This variant increased GOT2 activity and expression, and caused alterations in Krebs cycle metabolite ratios, both in tumors and in GOT2 KD cells transfected with the variant, suggesting *GOT2* is involved in PCC/PGL predisposition. In addition, we found a truncating germline *IDH3B* mutation in a patient with a PGL showing an altered α -ketoglutarate/isocitrate ratio. This study further attests to the relevance of the Krebs cycle in the development of PCC/PGL, some of which might be effectively treated with DNA demethylating agents.

Abstract

Purpose: Mutations in Krebs cycle genes are frequently found in patients with pheochromocytomas/paragangliomas. Disruption of SDH, FH or MDH2 enzymatic activities lead to accumulation of specific metabolites, which give rise to epigenetic changes in the genome that cause a characteristic hypermethylated phenotype. Tumors showing this phenotype, but no alterations in the known predisposing genes, could harbor mutations in other Krebs cycle genes.

Experimental Design: We used downregulation and methylation of *RBP1*, as a marker of a hypermethylation phenotype, to select eleven pheochromocytomas and paragangliomas for targeted exome sequencing of a panel of Krebs cycle-related genes. Methylation profiling, metabolite assessment and additional analyses were also performed in selected cases.

Results: One of the eleven tumors was found to carry a known cancer-predisposing somatic mutation in *IDH1*. A variant in *GOT2*, c.357A>T, found in a patient with multiple tumors, was associated with higher tumor mRNA and protein expression levels, increased GOT2 enzymatic activity in lymphoblastic cells, and altered metabolite ratios both in tumors and in GOT2 knock-down HeLa cells transfected with the variant. Array methylation-based analysis uncovered a somatic epigenetic mutation in *SDHC* in a patient with multiple pheochromocytomas and a gastrointestinal stromal tumor. Finally, a truncating germline *IDH3B* mutation was found in a patient with a single paraganglioma showing an altered α -ketoglutarate/isocitrate ratio.

Conclusions: This study further attests to the relevance of the Krebs cycle in the development of PCC and PGL, and points to a potential role of other metabolic enzymes involved in metabolite exchange between mitochondria and cytosol.

Introduction

Despite their low prevalence, pheochromocytomas (PCCs) and paragangliomas (PGLs) represent a paradigm for hereditary cancer due to the highest degree of heritability of these tumors among all human neoplasms (1). Up to 40% of individuals with PCC and/or PGL have a hereditary background due to germline mutations affecting one of thirteen susceptibility genes (2-13). The mutations result in two broad groups of tumors characterized by either activation of hypoxia or kinase receptor signaling pathways (1). Furthermore, somatic mutations in several of these genes or in two other PCC/PGL predisposition genes, *HIF2A* and *HRAS* (14, 15), are found in an additional ~30% of tumors (16). Finally, the presence of features of heritability amongst some of the patients without germline mutations in the known susceptibility genes, strongly suggests the implication of additional genes in this multi-genetic disease. Of note, more than half of the PCC/PGL predisposition genes encode enzymes involved in the Krebs cycle (*SDHA*, *SDHB*, *SDHC*, *SDHD*, *SDHAF2*, *FH* and *MDH2*), which stresses the crucial role of this pathway in PCC/PGL development and suggests that alterations in other genes from this pathway could account for more patients. This is even more likely for cases showing a noradrenergic or dopaminergic phenotype, which is associated with the presence of mutations in the aforementioned Krebs cycle-related genes.

In recent years, the application of high-throughput “omics” technologies to PCC/PGL research has led to improved understanding of the biology of these tumors, and paved the way for discovery of new predisposing genes (7, 12, 17). It has been known for years that pseudo-hypoxic PCCs/PGLs, such as SDH- and VHL-mutated tumors, share a similar transcriptional profile (18) that can be further segregated into different gene expression signatures (19). More recently, high-throughput methylation studies performed in PCCs/PGLs have revealed a particular CpG island methylation phenotype (CIMP) associated with the presence of Krebs cycle gene (*SDH*, *FH* or *MDH2*) mutations (11, 12). This CIMP profile is caused by impaired histone demethylation and 5-mC hydroxylation (5-hmC) due to the enzymatic inhibition of multiple α -KG-dependent dioxygenases by the accumulation of succinate and fumarate (20). In

addition, mutations in other Krebs cycle-related genes (*IDH1* and *IDH2*) also lead to a similar CIMP in gliomas (21), caused in this case by the accumulation of D-2-hydroxyglutarate (22). *IDH1* has been also found to be somatically mutated in two PGLs (23, 24). Though the majority of genes that define the altered methylation profile in PCC/PGL and gliomas are different, a substantial percentage of them (~25%) are silenced in both neoplasias (12). That is the case for *RBP1*, which is consistently methylated and downregulated in both types of tumors carrying Krebs cycle mutations (11, 25). Tumors carrying mutations in other PCC/PGL susceptibility genes, such as *RET*, *NF1*, *MAX* or *TMEM127*, all belonging to the so-called expression cluster 2, do not exhibit methylation of *RBP1* (11).

In the present study we use the low expression of *RBP1* as a marker of hypermethylation to select PCCs and PGLs as candidates for targeted exome sequencing of a panel of Krebs cycle-related genes in order to find new PCC/PGL predisposition genes.

Materials and Methods

Samples

Forty-nine tumors from patients showing noradrenergic or dopaminergic catecholamine phenotypes or no evidence of catecholamine production (when available), and testing negative for mutations in the major susceptibility genes (including all known PCC/PGL Krebs cycle-related genes: SDH, *FH* and *MDH2*), were included in the study. Immunostaining of SDHB was performed when formalin-fixed paraffin-embedded (FFPE) tissues were available, in order to rule out hidden mutations affecting the SDH genes, since negative SDHB immunohistochemistry is associated with the presence of SDH gene mutations in PCC/PGL (26, 27). The Instituto de Salud Carlos III (ISCIII) ethics committee approved the study, and all the patients provided written informed consent.

Quantitative real-time PCR

Total RNA was obtained from FFPE or from frozen material using the RNeasy FFPE (Qiagen) or TriReagent (MRC) kit, respectively, according to the manufacturers' instructions. cDNA was prepared from 1 µg of total RNA using oligo (dT) primers and SuperScript® III RT (Invitrogen). RBP1, SDHC and GOT2 mRNA levels were determined by quantitative PCR on a 7500 fast real-time PCR system (Applied Biosystems) using the Universal ProbeLibrary set (<https://www.roche-applied-science.com>), as described by the manufacturer. Relative mRNA levels were estimated by the 2-CT method (28) and normalized using β -actin (ACTB) as housekeeping gene. The results are shown as mean+s.d. ($n \geq 3$). mRNA obtained from tumors carrying mutations in other known pheochromocytoma susceptibility genes were used as controls. Tumors with RBP1 expression below 15 relative units (RU) ($n=14$) were considered candidates for subsequent analyses.

Pyrosequencing

Specific primers were used for PCR amplification and sequencing using the PyroMark assay (design version 2.0.01.15) in order to interrogate the methylation status of CpG sites from *RBP1*, as previously described (11).

Targeted next-generation sequencing

DNA extracted from 11 selected tumor samples was sequenced for a set of genes involved in the Krebs cycle by TruSight sequencing technology (Illumina), which comprises oligo probes targeting the genes of interest. The makeup of the panel was planned to cover the complete coding region of thirty seven human genes found to be directly or indirectly involved in the Krebs cycle based on the KEGG (<http://www.genome.jp/kegg/pathway.html>) and Genecard (<http://www.genecards.org/>) databases (Supplementary Table S1). *Designstudio* software (Illumina) was used to design the 733 amplicons included in the panel (cumulative Target: 65525 bp and coverage of 99%). This tool avoids designing for amplification primers that include known polymorphisms. Once the library was prepared following the manufacturer's instructions, next-generation sequencing was performed using MiSeq desktop sequencer (Illumina) and sequence alignment was carried out using *MiSeq Reporter* and *Illumina VariantStudio* softwares (Illumina). Variant calling was performed using GATK and *Somatic Variant Caller*, and identified variants were filtered considering mapping quality, variant score, depth, strand bias and annotation quality. In order to establish a cutoff to consider a nucleotide substitution reported in controls as a candidate pathogenic variant, we used publically available data for *SDHB* germline mutations since they have the lowest penetrance amongst mutations in the known PCC/PGL susceptibility genes (29). The highest frequency for a known pathogenic *SDHB* mutation, found in the Genome Aggregation Consortium (gnomAD) database (<http://gnomad.broadinstitute.org/>), was 1.805×10^{-5} , which was therefore applied as the cutoff.

Targeted regions without appropriate coverage and quality or with low mappability were re-amplified by Sanger sequencing. The PredictSNP consensus classifier (30) was used to predict the effect of the substitutions that passed all filtering steps. Tumor DNA samples from a series of 63 unselected patients with PCC or PGL, and negative for germline mutations in the known susceptibility genes, were tested by targeted next-generation sequencing for the presence of mutations in TCA-related genes.

Methylation assay and data processing

DNA was extracted and purified from the 11 selected cases, and from five SDH gene-mutated controls (two *SDHB*, one *SDHA*, one *SDHD*, and one *SDHC*-mutated tumors), using the DNeasy Blood & Tissue Kit (Qiagen) according to manufacturer's recommendations. Bisulfite conversion of DNA was performed using the EZ DNA Methylation Kit (Zymo Research) and genome-wide DNA methylation was assayed using the Infinium HumanMethylation450 BeadChip (Illumina) at the *Centro Nacional de Genotipado* (CEGEN-ISCIII), as previously described (31). This BeadChip interrogates more than 485,000 methylation sites per sample. Beta values for each interrogated CpG were assigned using the Genome Studio Methylation module. Methylomes from the 19 tumors were profiled together with 13 additional controls (four non-SDH gene-mutated and nine SDH gene-mutated tumors) obtained from the GEO database (accession number GSE43298). We used the clustering average for linkage and City-block as the distance measure, and assumed a standard deviation of 0.22.

Immunohistochemistry

Immunohistochemical SDHB (HPA002868, Sigma) analysis of 3 μ m formalin-fixed paraffin-embedded (FFPE) tissues was used for all cases, where tissue was available, to further rule out the presence of SDH gene mutations, as previously reported (26). Specific

immunohistochemical staining of GOT2 (NBP1-80521, Novus) was performed using FFPE sections from the two available *GOT2*-mutated tumors, following standard procedures; five tumors carrying mutations in PCC susceptibility genes were used as controls. Finally, immunohistochemical staining of 5-hmc (Active Motif; 39770) was performed using 3 µm FFPE sections from the *IDH3B*-mutated tumors, following standard procedures.

Enzymatic activity analyses

Cytosolic and mitochondrial fractions were obtained after processing of lymphoblastoid cells obtained from the *GOT2*-mutation carrier and from three controls, as previously described (32). Protein concentration was determined using Bradford method with bovine serum albumin as standard. The cytosolic and mitochondrial fractions were used to determine the enzymatic activity of GOT1 and GOT2, quantified as a decrease in NADH fluorescence, after the addition of aspartate, using a BMG plate reader, as previously described (33). Control and mutant *GOT* activity in cell fractions were measured in duplicate at different dilutions in 3 independent paired experiments. Lactate dehydrogenase (LDH, measured as the increase in NADH caused by lactate addition) and citrate synthase (CS, measured as the increase in absorption of 5,5'-dithiobis-2-nitrobenzoic acid after the addition of OAA) were assayed using standard procedures (33, 34). GOT2 activity was corrected by subtracting the estimated cytosolic contamination (% of LDH present) from the activity measured in the mitochondrial fraction.

Mutagenesis

GOT2 c.357A>T and c.223T>G variants and the *OGDHL* c.750G>T substitution were generated by mutagenesis using the QuikChange II Site-Directed Mutagenesis Kit (Stratagene, La Jolla, CA, USA), according to the manufacturer's instructions. Wild-type and mutagenized inserts were verified by sequencing both strands.

Cell cultures

Lymphocytes from the carrier of the c.357A>T *GOT2* mutation were immortalized using Epstein-Barr virus (EBV), as previously described (35). HeLa cell line (kindly provided by Flow Cytometry Core Unit, CNIO, Madrid) was authenticated by short tandem repeat profiling (GenePrint® 10 System, Promega) and periodically confirmed to be mycoplasma free by qPCR. HeLa cells, used within ten passages after authentication, were cultured in Dulbecco's modified Eagle medium Gluta MAX (DMEM; Invitrogen), supplemented with 10% (v/v) foetal bovine serum (FBS, PAA laboratories), 1% (v/v) penicillin/streptomycin and 0.6% (v/v) Fungizone (Gibco), and maintained at 37°C in a humidified incubator with 5% CO₂. MISSION® shRNA lentiviral transduction particles were used to specifically knockdown *GOT2* (TRCN0000034827; Sigma) and *OGDHL* (TRCN0000426732; Sigma). Stable gene knockdown (KD) was established by cellular resistance to puromycin (1 µg/ml). Scrambled non-target shRNA control vectors served as negative controls. HeLa (*GOT2* or *OGDHL*) KD cells were seeded at 550,000 cells per well on 6-well plates for 24h. Each well was transiently transfected with 2 µg of pCMV6-AC plasmid containing the full cDNA sequence of *GOT2* (SC127269, Origene), or *OGDHL* (RC205225, Origene), or with 2 µg of pCMV6-AC plasmids carrying the corresponding variant (*GOT2* c.357A>T and c.223T>G, or *OGDHL* c.750G>T) using Lipofectamine 2000 (Invitrogen), according to the manufacturer's recommendations. pCMV6-AC empty vector (EV) was used as a control. In the proliferation assay, *GOT2* KD HeLa cells were transfected with EV, *GOT2*-WT or *GOT2*-c.357A>T cDNA, and were seeded 24 hours post-transfection at 30,000 cells per well on 12-well plates. Then, cells were trypsinized and counted after 48h, 72h and 96h post-transfection.

Western blot

To demonstrate the absence of full-length GOT2 or OGDHL proteins in KD HeLa cells, we performed western blot analysis using polyclonal rabbit anti-GOT2 (NBP1-80521; Novus) and anti-OGDHL (NBP1-91486; Novus) antibodies. Proteins were separated by 10% SDS-PAGE and transferred to a polyvinylidene fluoride membrane. The membrane was blocked and then incubated with a 1:2,000 or a 1:1,000 dilution of GOT2 and OGDHL respectively, following the manufacturer's instructions. Equal protein loading was assessed using a 1:12,000 dilution of monoclonal anti- β -actin mouse antibody (A5441, Sigma-Aldrich).

Liquid chromatographic tandem-mass spectrometric determination of metabolites

Fresh frozen or FFPE tumor tissue (5-10 mg) from available selected cases and from 15 controls, was immersed in 500 μ l LC/MS grade methanol containing isotope-labeled internal standards and processed as previously described (11). For cell cultures, 500,000 cells were cultured, washed 4 times with PBS and extracted in methanol containing isotope-labeled internal standards. Analysis of metabolites was carried out using an AB Sciex 5500 QTRAP mass spectrometer coupled to an Acquity ultra-high performance liquid chromatographic system (Waters), as previously described (11).

Results

Clinical and molecular features of cases showing downregulation and methylation of RBP1

Fourteen out of the 49 tumors analyzed by qPCR showed low (lower than 15 RU) or almost no RBP1 expression levels compared to the remaining 35 assessed tumors and ten control tumors carrying mutations in PCC/PGL susceptibility genes (Supplementary Fig. S1A). Pyrosequencing analysis confirmed gene methylation as the cause of the *RBP1* downregulation in 11 out of the 14 tumors, and therefore further analysis were focused on these 11 cases. Five of the 11 patients had multiple PCCs/PGLs, one of them suffering also from a gastrointestinal stromal tumor (GIST), and one case showed distant metastases (Table 1). Nine cases showed a positive immunostaining for SDHB which ruled out the presence of SDH gene causal mutations in these patients. Only one H&N PGL developed by the patient who also suffered from GIST tested negative (Supplementary Fig. S1B), suggesting that a hidden SDH gene alteration could account for this patient.

Next-generation sequencing findings

Five missense variants, affecting four genes and detected in three samples, passed the filtering process after excluding variants found at a frequency $>2.471 \times 10^{-5}$ of controls in gnomAD (Table 1). Sanger sequencing was used to validate both the presence of the variants in the corresponding tumor (Fig. 1A), and the presence/absence of the variant in the germline of the patients. All variants were found in the germline of the corresponding patient, with the exception of the c.394C>T *IDH1* somatic mutation. Three variants were predicted to be deleterious and two neutral by PredictSNP (data not shown).

Seven variants (six missense and one frameshift), affecting four genes and found in seven samples, were detected and validated in the extended series of 63 tumors. When we applied the same filtering process to that used for the selected series of tumors, only a novel *IDH3B* truncating mutation remained (Fig. 1B). The variant was found in the germline of a patient with a single non-secreting jugular PGL at age 51 years.

Methylation profiling classified most tumors within the CIMP cluster

Methylomes from 16 tumors (11 selected cases and five *SDH* gene-mutated controls) were profiled together with methylomes from 13 additional genotyped PCCs/PGLs obtained from GEO. Ten RBP1-downregulated and methylated tumors showed a “CIMP-like” profile similar to that observed for PCC/PGLs carrying *SDH* gene mutations, whereas only one case clustered with hypomethylated tumors carrying mutations in *NF1*, *RET* or *MAX* (Fig. 1C). When we focused on the methylation status of the Krebs cycle genes included in the panel, a tumor (Tumor_4 in Table 1) was found to show significantly higher methylation levels for 11 CpG targets encompassing the *SDHC* promoter region in 1q23.3 (Fig. 2A). In order to test for constitutional *SDHC* methylation in the patient, we analyzed DNA obtained from blood and found no silencing of the *SDHC* locus (Supplementary Fig. S1C). Absence of *SDHC* mRNA expression was demonstrated by qPCR for the tumor exhibiting methylation of the *SDHC* promoter, compared to controls (Fig. 2B). Of note, and as mentioned above, the *SDHC*-methylated tumor was the only one from our series that showed negative SDHB immunohistochemistry. Finally, the methylome from the *IDH3B*-mutated tumor also showed a “CIMP-like” profile (data not shown), further supported by a negative 5-hmC immunohistochemistry (Supplementary Fig. S1D).

Higher GOT2 expression and activity in tissues carrying the c.357A>T mutation

Since we found two different variants in *GOT2* in two different cases, and both tumors were grouped within the “CIMP-like” cluster, we assessed the expression of the gene in the tumors. Two available tumors from the patient carrying the *GOT2* c.357A>T variant (Fig. 3A) showed a significantly higher *GOT2* mRNA expression (Fig. 3B), as well as a granular cytoplasmic differential immunostaining, compared to controls (Fig. 3C). Tumor_1 which carried the other *GOT2* variant, c.223T>G, showed normal *GOT2* expression. EBV-immortalized lymphoblastoid cells carrying the c.357A>T *GOT2* mutation exhibited significantly higher *GOT2* enzymatic activity compared to three *GOT2*-wild type lymphoblastoid cell lines (Fig. 3D).

Tumoral metabolite ratios

Liquid chromatographic tandem-mass spectrometric was applied to all available tissues to assess whether the tumors carrying the identified variants showed significant alterations in the metabolites of the Krebs cycle. Amongst the 10 cases tested (Tumor_9 could not be analyzed) only the tumors carrying the *GOT2* c.357A>T variant (Tumor_2) and the *OGDHL/PCK2* variations (Tumor_3), showed a high succinate/fumarate ratio (Fig. 4A) similar to that observed for SDH gene-mutated tumors. This abnormal succinate/fumarate ratio was not associated with SDH alterations in either of the two tumors, since they resulted positive for SDHB immunohistochemistry (Table 1). In addition, the tumor carrying the *IDH1* c.394C>T mutation, showed an elevated hydroxyglutarate/isocitrate ratio compared to controls (n=8) (Fig. 4B), which is consistent with the presence of pathological *IDH1/2* mutations. None of the other tumors (those not carrying these variants) had altered metabolite ratios. The *IDH3B*-mutated tumor showed an elevated α -ketoglutarate/isocitrate ratio compared to controls (Fig. 4C).

c.357A>T *GOT2* introduction in *GOT2* KD cells increased metabolite ratios

To demonstrate the relevance of the c.357A>T variant in GOT2 enzymatic activity, we first silenced GOT2 (GOT2 KD) by shRNA in HeLa cells (Supplementary Fig. S2A). Subsequent transient introduction of GOT2 cDNA carrying the variant c.357A>T in GOT2 KD cells triggered a slight increase in the succinate/fumarate ratio and a significant increase of α -ketoglutarate/citrate and aspartate/glutamate ratios, compared to GOT2 KD cells transfected with wild-type GOT2 cDNA (Fig. 4D and E). Moreover, the growth rate of GOT2 KD cells transfected with c.357A>T-GOT2 was higher (although not significantly so) than that observed for GOT2 KD cells transfected with WT-GOT2, and significantly higher than that observed for KD cells (Supplementary Fig. S2B). Further, GOT2 KD cells transfected with the c.223T>G variant showed aspartate/glutamate ratios similar to the control (Supplementary Fig. S3A).

Depletion of OGDHL had no effect on metabolite ratios

No alteration in the succinate/fumarate ratio was observed after silencing *OGDHL* in HeLa cells by shRNA, or after transient introduction of the c.750G>T variant in KD cells (Supplementary Fig. S3B). Silencing *PCK2* in HeLa cells was not possible either by shRNA or CRISPR-Cas9 technologies (data not shown).

Discussion

PCC/PGL are paradigmatic for illustrating the importance of human genetics in cancer, not only because of the high degree of heritability of the tumors and involvement of a large number of genes (more than 13), but also because these tumors are the main manifestation of genetic alterations in *SDHD*. *SDHD* is a gene that went down in history as the first metabolic gene involved in the Krebs cycle and the respiratory chain whose mutations were associated with the development of cancer. Since then, mutations affecting six additional genes involved in the Krebs cycle energy pathway have been associated with the development of PCC/PGL and with a particular hypermethylation phenotype. Herein we describe how the selection of samples based on the expression of a methylation marker, identifies PCCs/PGLs harboring candidate variants affecting other Krebs cycle-related genes. These results highlight both the relevance of this pathway in PCC/PGL development and the need for marker-based selection of samples for the discovery of cancer susceptibility genes in order to avoid genetic heterogeneity.

To date, only two studies have focused on the involvement of *IDH1/2* in PCC/PGL development, yielding 1/365 and 0/104 tumors carrying a pathogenic mutation affecting *IDH1* (23). Another *IDH1* mutation has also been identified in one PGL among 173 samples from The Cancer Genome Atlas (<http://www.cbioportal.org/index.do>) (24), which further confirms the low frequency of alterations affecting this gene in PCC/PGL. The two mentioned *IDH1* mutations, as well as the one reported herein, affect the same amino acid (p.Arg132Cys) and were found in older patients (>61 years) with PGLs, which stresses the relevance of this cancer-prone alteration to extra-adrenal tumors. The accumulation of hydroxyglutarate observed in the tumor, and the absence of any other somatic or germline alteration in the known PCC/PGL susceptibility genes, confirmed the driver role of the *IDH1* mutation in this case and explains its CIMP profile.

Glutamic-oxaloacetic transaminase 2 (GOT2) is a mitochondrial enzyme that plays a role in amino acid metabolism and the urea and Krebs cycles. GOT2 converts oxaloacetate into

aspartate by transamination, with the consequent conversion of glutamate to α -ketoglutarate. In SDH-deficient cells, glutamine and glutamate are used to provide metabolic intermediates to the truncated Krebs cycle, after conversion to α -ketoglutarate by GOT2 or GLUD1 enzymes (36, 37). It has been recently described that lysine acetylation of GOT2 enhances the protein association between GOT2 and MDH2, stimulating the malate shuttle activity and thus promoting pancreatic cell proliferation and tumor growth *in vivo* (38). Mutant *KRAS* promotes the reprogramming of glutamine metabolism in pancreatic cancer through GOT1/GOT2-mediated transamination pathway (39).

Both the expression of GOT2 and its enzymatic activity found in c.357A>T-mutated tissues suggest an activating role of the mutation. Moreover, the high succinate/fumarate ratio observed in the *GOT2*-mutated tumor, as well as the slight increment of α -ketoglutarate compared to controls, could be explained by an excess of this latter metabolite due to the higher enzymatic activity of GOT2. Introduction of the mutated p.Glu119Asp variant, but not p.Tyr75Asp, in GOT2 KD HeLa cells recapitulates the accumulation of metabolites observed in tumors carrying the variant, and increases cell proliferation. Interestingly, GOT2 knockdown led to an accumulation of glutamate as well as to significantly lower levels of Krebs cycle metabolites fumarate and malate in melanoma cells (40). Thus, it seems plausible that a higher activity of GOT2 could lead to an increment of anaplerotic incorporation of α -ketoglutarate to the Krebs cycle and hence to the oncogenic accumulation of succinate. The absence of *GOT2* variants in unselected cases suggests their prevalence is low in PCC/PGL patients, which has also reported for other TCA-related genes (11, 41).

The presence of aberrant hypermethylation of *SDHC* has been reported to be a novel mechanism of tumor development in Carney triad (PGL, GIST and pulmonary chondroma) patients (42). Moreover, epimutations in *SDHC* have also been reported in hypermethylated SDH-deficient GISTs (43), mainly associated with Carney triad. Interestingly, in both studies the aberrant methylation of *SDHC* occurred exclusively in females. Recently, epigenetic mutation of the *SDHC* promoter has been found in another female with two PGLs (44). As far as we know,

the case reported in the present study is the first example of a *SDHC* epimutation affecting a patient with Carney-Stratakis syndrome (co-occurrence of PGL and GIST). Regarding the mechanism involved in silencing *SDHC*, a potential role of sex chromosome or hormone biology has been proposed (43). The patient described herein is a female, and this explanation could also account for this case. The complete absence of *SDHC* expression in the tumor suggested that, in addition to the observed hemi-methylation, a second hit affecting the gene was also present. High-density SNP genotyping performed in the tumor showing *SDHC* methylation revealed no alterations affecting chromosome 1, where *SDHC* is located (data not shown). Furthermore, the tumor had a normal DNA copy number profile, which is consistent with previous findings describing that DNA copy number changes are infrequent in parasympathetic PGLs (45). The absence of high succinate/fumarate ratio in this tumor could be due to the lower reliability of measurements of these metabolites in H&N PGLs (46), presumably due to a higher content of stromal cells diluting the signal from tumor cells. The absence of aberrant hypermethylation in known susceptibility genes in the other tumors analyzed (Supplementary Fig. S4) suggests that this mechanism is extremely rare in PCC/PGL.

The altered succinate/fumarate ratio observed in a tumor carrying two rare variants in *OGDHL* and *PCK2* suggested that either gene could be involved in the disease. Interestingly, the promoter of *OGDHL* is differentially methylated in different tissue types, and it is thought that inactivation of *OGDHL* can contribute to cervical tumorigenesis (47). On the other hand, the mitochondrial phosphoenolpyruvate carboxykinase (*PCK2*) is an enzyme involved in gluconeogenesis, converting oxaloacetate into phosphoenolpyruvate, which also has a cataplerotic function, maintaining metabolic flux through the Krebs cycle by removing excess oxaloacetate. It has been reported that *PCK2* activation mediates an adaptive response to glucose depletion in lung cancer (48). Although we have ruled out a link between *OGDHL* depletion and an altered succinate/fumarate ratio, we were not able to demonstrate the relevance of *PCK2* in PCC/PGL development.

Homozygous loss-of-function mutations in *IDH3B* have been found in two families with retinitis pigmentosa (49), and somatic mutations in *IDH3B* have been recently found in acute myeloid leukemia (50). *IDH3B* encodes the beta subunit of NAD-specific isocitrate dehydrogenase 3 (IDH3), which is involved in the oxidation of isocitrate to α -ketoglutarate in the Krebs cycle. It has been demonstrated that IDH3 activity in lysates from cells carrying heterozygous truncating *IDH3B* mutations was only 24% of that observed in normal controls (49). In addition, the altered α -ketoglutarate/isocitrate ratio detected in the tumor carrying the truncating mutation, and the associated CIMP-like profile further suggest a causative role for this variant in PGL development.

In summary, based on our selection of cases for exome sequencing of Krebs cycle genes and whole-genome DNA methylation assessment, we have identified rare pathological alterations in known PCC/PGL susceptibility genes (*SDHC* and *IDH1*), and two new candidate genes possibly involved in the hereditary predisposition (*GOT2* and *IDH3B*). This study further strengthens the evidence for the relevance of the Krebs cycle in the development of PCC and PGL, and points to other enzymes involved in metabolite exchange between mitochondria and cytosol.

References

1. Dahia PL. Pheochromocytoma and paraganglioma pathogenesis: learning from genetic heterogeneity. *Nat Rev Cancer* 2014;14:108-19.
2. Astuti D, Latif F, Dallol A, Dahia PL, Douglas F, George E, et al. Gene mutations in the succinate dehydrogenase subunit SDHB cause susceptibility to familial pheochromocytoma and to familial paraganglioma. *Am J Hum Genet* 2001;69:49-54.
3. Burnichon N, Briere JJ, Libe R, Vescovo L, Riviere J, Tissier F, et al. SDHA is a tumor suppressor gene causing paraganglioma. *Hum Mol Genet* 2010;19:3011-20.
4. Baysal BE, Ferrell RE, Willett-Brozick JE, Lawrence EC, Myssiorek D, Bosch A, et al. Mutations in SDHD, a mitochondrial complex II gene, in hereditary paraganglioma. *Science* 2000;287:848-51.
5. Latif F, Tory K, Gnarr J, Yao M, Duh FM, Orcutt ML, et al. Identification of the von Hippel-Lindau disease tumor suppressor gene. *Science* 1993;260:1317-20.
6. Mulligan LM, Kwok JB, Healey CS, Elsdon MJ, Eng C, Gardner E, et al. Germ-line mutations of the RET proto-oncogene in multiple endocrine neoplasia type 2A. *Nature* 1993;363:458-60.
7. Qin Y, Yao L, King EE, Buddavarapu K, Lenci RE, Chocron ES, et al. Germline mutations in TMEM127 confer susceptibility to pheochromocytoma. *Nat Genet* 2010;42:229-33.
8. Niemann S, Muller U. Mutations in SDHC cause autosomal dominant paraganglioma, type 3. *Nat Genet* 2000;26:268-70.
9. Wallace MR, Marchuk DA, Andersen LB, Letcher R, Odeh HM, Saulino AM, et al. Type 1 neurofibromatosis gene: identification of a large transcript disrupted in three NF1 patients. *Science* 1990;249:181-6.
10. Hao HX, Khalimonchuk O, Schraders M, Dephore N, Bayley JP, Kunst H, et al. SDH5, a gene required for flavination of succinate dehydrogenase, is mutated in paraganglioma. *Science* 2009;325:1139-42.
11. Cascon A, Comino-Mendez I, Curras-Freixes M, de Cubas AA, Contreras L, Richter S, et al. Whole-exome sequencing identifies MDH2 as a new familial paraganglioma gene. *J Natl Cancer Inst* 2015;107.
12. Letouze E, Martinelli C, Lorient C, Burnichon N, Abermil N, Ottolenghi C, et al. SDH mutations establish a hypermethylator phenotype in paraganglioma. *Cancer Cell* 2013;23:739-52.
13. Yang C, Zhuang Z, Fliedner SM, Shankavaram U, Sun MG, Bullova P, et al. Germ-line PHD1 and PHD2 mutations detected in patients with pheochromocytoma/paraganglioma-polycythemia. *J Mol Med (Berl)* 2015;93:93-104.
14. Crona J, Delgado Verdugo A, Maharjan R, Stalberg P, Granberg D, Hellman P, et al. Somatic mutations in H-RAS in sporadic pheochromocytoma and paraganglioma identified by exome sequencing. *J Clin Endocrinol Metab* 2013;98:E1266-71.
15. Zhuang Z, Yang C, Lorenzo F, Merino M, Fojo T, Kebebew E, et al. Somatic HIF2A gain-of-function mutations in paraganglioma with polycythemia. *N Engl J Med* 2012;367:922-30.
16. Curras-Freixes M, Inglada-Perez L, Mancikova V, Montero-Conde C, Leton R, Comino-Mendez I, et al. Recommendations for somatic and germline genetic testing of single pheochromocytoma and paraganglioma based on findings from a series of 329 patients. *J Med Genet* 2015.
17. Comino-Mendez I, Gracia-Aznarez FJ, Schiavi F, Landa I, Leandro-Garcia LJ, Leton R, et al. Exome sequencing identifies MAX mutations as a cause of hereditary pheochromocytoma. *Nat Genet* 2011;43:663-7.
18. Dahia PL, Ross KN, Wright ME, Hayashida CY, Santagata S, Barontini M, et al. A HIF1alpha regulatory loop links hypoxia and mitochondrial signals in pheochromocytomas. *PLoS Genet* 2005;1:72-80.
19. Lopez-Jimenez E, Gomez-Lopez G, Leandro-Garcia LJ, Munoz I, Schiavi F, Montero-Conde C, et al. Research resource: Transcriptional profiling reveals different pseudohypoxic signatures in SDHB and VHL-related pheochromocytomas. *Mol Endocrinol* 2010;24:2382-91.

20. Xiao M, Yang H, Xu W, Ma S, Lin H, Zhu H, et al. Inhibition of alpha-KG-dependent histone and DNA demethylases by fumarate and succinate that are accumulated in mutations of FH and SDH tumor suppressors. *Genes Dev* 2012;26:1326-38.
21. Turcan S, Rohle D, Goenka A, Walsh LA, Fang F, Yilmaz E, et al. IDH1 mutation is sufficient to establish the glioma hypermethylator phenotype. *Nature* 2012;483:479-83.
22. Dang L, White DW, Gross S, Bennett BD, Bittinger MA, Driggers EM, et al. Cancer-associated IDH1 mutations produce 2-hydroxyglutarate. *Nature* 2009;462:739-44.
23. Gaal J, Burnichon N, Korpershoek E, Roncelin I, Bertherat J, Plouin PF, et al. Isocitrate dehydrogenase mutations are rare in pheochromocytomas and paragangliomas. *J Clin Endocrinol Metab* 2010;95:1274-8.
24. Fishbein L, Leshchiner I, Walter V, Danilova L, Robertson AG, Johnson AR, et al. Comprehensive Molecular Characterization of Pheochromocytoma and Paraganglioma. *Cancer Cell* 2017;31:181-93.
25. Chou AP, Chowdhury R, Li S, Chen W, Kim AJ, Piccioni DE, et al. Identification of retinol binding protein 1 promoter hypermethylation in isocitrate dehydrogenase 1 and 2 mutant gliomas. *J Natl Cancer Inst* 2012;104:1458-69.
26. van Nederveen FH, Gaal J, Favier J, Korpershoek E, Oldenburg RA, de Bruyn EM, et al. An immunohistochemical procedure to detect patients with paraganglioma and pheochromocytoma with germline SDHB, SDHC, or SDHD gene mutations: a retrospective and prospective analysis. *Lancet Oncol* 2009;10:764-71.
27. Gill AJ, Benn DE, Chou A, Clarkson A, Muljono A, Meyer-Rochow GY, et al. Immunohistochemistry for SDHB triages genetic testing of SDHB, SDHC, and SDHD in paraganglioma-pheochromocytoma syndromes. *Hum Pathol* 2010;41:805-14.
28. Livak KJ, Schmittgen TD. Analysis of relative gene expression data using real-time quantitative PCR and the 2(-Delta Delta C(T)) Method. *Methods* 2001;25:402-8.
29. Schiavi F, Milne RL, Anda E, Blay P, Castellano M, Opocher G, et al. Are we overestimating the penetrance of mutations in SDHB? *Hum Mutat* 2010;31:761-2.
30. Bendl J, Stourac J, Salanda O, Pavelka A, Wieben ED, Zendulka J, et al. PredictSNP: robust and accurate consensus classifier for prediction of disease-related mutations. *PLoS Comput Biol* 2014;10:e1003440.
31. Bibikova M, Le J, Barnes B, Saedinia-Melnyk S, Zhou L, Shen R, et al. Genome-wide DNA methylation profiling using Infinium(R) assay. *Epigenomics* 2009;1:177-200.
32. Trounce IA, Kim YL, Jun AS, Wallace DC. Assessment of mitochondrial oxidative phosphorylation in patient muscle biopsies, lymphoblasts, and transmitochondrial cell lines. *Methods Enzymol* 1996;264:484-509.
33. Bergmeyer HU, Bergmeyer J, Grassl M. *Methods of enzymatic analysis / V. 3, Enzymes 1 oxidoreductases, transferases.* 3rd ed ed. Weinheim: Verlag Chemie; 1983.
34. Bergmeyer HU, Bergmeyer J, Grabl M. *Methods of enzymatic analysis. IV, Enzymes 2,. Esterases, glycosidases, lyases, ligases.* 3rd ed ed. Weinheim [etc.]: Verlagchemie; 1984.
35. Ausubel FM. *Current protocols in molecular biology.* New York: Greene Pub. Associates ; Wiley-Interscience; 1988. p. v. (loose-leaf).
36. Saxena N, Maio N, Crooks DR, Ricketts CJ, Yang Y, Wei MH, et al. SDHB-Deficient Cancers: The Role of Mutations That Impair Iron Sulfur Cluster Delivery. *J Natl Cancer Inst* 2016;108.
37. Lussey-Lepoutre C, Hollinshead KE, Ludwig C, Menara M, Morin A, Castro-Vega LJ, et al. Loss of succinate dehydrogenase activity results in dependency on pyruvate carboxylation for cellular anabolism. *Nat Commun* 2015;6:8784.
38. Yang H, Zhou L, Shi Q, Zhao Y, Lin H, Zhang M, et al. SIRT3-dependent GOT2 acetylation status affects the malate-aspartate NADH shuttle activity and pancreatic tumor growth. *EMBO J* 2015;34:1110-25.
39. Son J, Lyssiotis CA, Ying H, Wang X, Hua S, Ligorio M, et al. Glutamine supports pancreatic cancer growth through a KRAS-regulated metabolic pathway. *Nature* 2013;496:101-5.
40. Ratnikov B, Aza-Blanc P, Ronai ZA, Smith JW, Osterman AL, Scott DA. Glutamate and asparagine cataplerosis underlie glutamine addiction in melanoma. *Oncotarget* 2015;6:7379-89.

41. Bayley JP, Kunst HP, Cascon A, Sampietro ML, Gaal J, Korpershoek E, et al. SDHAF2 mutations in familial and sporadic paraganglioma and pheochromocytoma. *Lancet Oncol* 2010;11:366-72.
42. Haller F, Moskalev EA, Faucz FR, Barthelmess S, Wiemann S, Bieg M, et al. Aberrant DNA hypermethylation of SDHC: a novel mechanism of tumor development in Carney triad. *Endocr Relat Cancer* 2014;21:567-77.
43. Killian JK, Miettinen M, Walker RL, Wang Y, Zhu YJ, Waterfall JJ, et al. Recurrent epimutation of SDHC in gastrointestinal stromal tumors. *Sci Transl Med* 2014;6:268ra177.
44. Richter S, Klink B, Nacke B, deCubas AA, Mangelis A, Rapizzi E, et al. Epigenetic mutation of the succinate dehydrogenase C promoter in a patient with two paragangliomas. *J Clin Endocrinol Metab* 2015;jc20153856.
45. Dannenberg H, de Krijger RR, Zhao J, Speel EJ, Saremaslani P, Dinjens WN, et al. Differential loss of chromosome 11q in familial and sporadic parasympathetic paragangliomas detected by comparative genomic hybridization. *Am J Pathol* 2001;158:1937-42.
46. Richter S, Peitzsch M, Rapizzi E, Lenders JW, Qin N, de Cubas AA, et al. Krebs cycle metabolite profiling for identification and stratification of pheochromocytomas/paragangliomas due to succinate dehydrogenase deficiency. *J Clin Endocrinol Metab* 2014;99:3903-11.
47. Sen T, Sen N, Noordhuis MG, Ravi R, Wu TC, Ha PK, et al. OGDHL is a modifier of AKT-dependent signaling and NF-kappaB function. *PLoS One* 2012;7:e48770.
48. Leithner K, Hrzenjak A, Trotschmuller M, Moustafa T, Kofeler HC, Wohlkoeinig C, et al. PCK2 activation mediates an adaptive response to glucose depletion in lung cancer. *Oncogene* 2015;34:1044-50.
49. Hartong DT, Dange M, McGee TL, Berson EL, Dryja TP, Colman RF. Insights from retinitis pigmentosa into the roles of isocitrate dehydrogenases in the Krebs cycle. *Nat Genet* 2008;40:1230-4.
50. Garg M, Nagata Y, Kanojia D, Mayakonda A, Yoshida K, Haridas Keloth S, et al. Profiling of somatic mutations in acute myeloid leukemia with FLT3-ITD at diagnosis and relapse. *Blood* 2015;126:2491-501.

Table 1. Clinical and genetic findings of studied cases

ID	Tumor_ 1	Tumor_ 2	Tumor_ 3	Tumor_ 4	Tumor_ 5	Tumor_ 6	Tumor_ 7	Tumor_ 8	Tumor_ 9	Tumor_ 10	Tumor_ 11		
Gene(s) altered	<i>IDH1</i>	<i>GOT2</i>	<i>GOT2</i>	<i>OGDHL</i>	<i>PCK2</i>	-	-	-	-	-	-	-	
DNA variant	c.394C>T	c.223T>G	c.357A>T	c.750G>T	c.1742C>T	-	-	-	-	-	-	-	
Protein change	p.Arg132 Cys	p.Tyr75 Asp	p.Glu119 Asp	p.Arg250 Ser	p.Ala581 Val	-	-	-	-	-	-	-	
Frequency in gnomAD	Not found	3/246192	2/277174	Not found	2/246224	-	-	-	-	-	-	-	
Frequency in Spaniards*	0/816	0/816	0/816	0/816	0/816	-	-	-	-	-	-	-	
PredictSNP	Del	Del	Neutral	Neutral	Del	-	-	-	-	-	-	-	
Methylation cluster	CIMP		CIMP	non-CIMP		CIMP	CIMP	CIMP	non- CIMP	CIMP	CIMP	CIMP	CIMP
SDHB IHC	positive		positive	positive		negative	positive	positive	positive	positive	NA	positive	positive
Metabolites	H		S/F	S/F		-	-	-	-	-	NA	-	-
Location	TAP		TAP	PCC		H&N	H&N	H&N	H&N	H&N	H&N	H&N	TAP
Biochemical Phenotype	NM		D	NM		NM, D	NS	NM	U	U	NS	NS	NM
Number of tumors	S		M (n=9)	S		M (n=3), GIST	M (n=2)	M (n=5)	S	S	S	S	M (n=3)
Clinical Behaviour	B		Mg	B		B	B	B	U	B	U	B	B

Del, deleterious; *: CIBERER Spanish exome database (<http://csvs.babelomics.org/>); NA, not available; H, high hydroxyglutarate levels; S/F, high succinate/fumarate ratio; TAP, thoracic-abdominal PGL, PCC, pheochromocytoma, H&N, head and neck PGL; NM, normetanephrine; D, dopamine; NS, predominant secretion not specified; U, unknown; S, single; M, multiple; GIST, gastrointestinal stromal tumor; B, benign; Mg, malignant.

Figures Legends

Figure 1. (A) Sanger sequencing validation (in tumor DNA) of targeted exome findings. (B) Sanger sequencing validation (in tumor DNA) of the *IDH3B* mutation found in the extended series. (C) Hierarchical clustering of the 11 pheochromocytomas/paragangliomas showing *RBP1* mRNA downregulation, as well as SDH gene-mutated and non-SDH gene-mutated controls. Tumors hybridized and analyzed in the present study are denoted in black letters, while tumors downloaded from GEO are denoted in grey. Two clusters were observed and named CIMP (including all SDH gene-mutated controls), and non-CIMP (including all non-SDH gene-mutated controls). Tumor_3: tumor carrying the *OGDHL* and *PCK2* variants; tumor_2: tumor carrying the c.357A>T *GOT2* variant and tumor_1: tumor carrying the *IDH1* and the c.223T>G *GOT2* variants.

Figure 2. (A) DNA methylation (M_values) for 17 CpG island probes located within the *SDHC* locus in the 11 analyzed tumors, compared to IVD (*in vitro* methylated DNA). The results of the immunostaining for SDHB (SDHB IHC) are also represented. NA: not available. (B) mRNA expression of *SDHC* in the *SDHC*-methylated tumor (tumor_4) compared to controls (n=5). Error bars represent standard deviations.

Figure 3. (A) *GOT2* c.357A>T variant in the germline and in two tumors from the patient revealed by Sanger sequencing. The asterisk marks the tumor subjected to exome sequencing. (B) *GOT2* mRNA expression in two tumors (tumor_2A and tumor_2B) carrying the *GOT2* c.357A>T variant, compared to controls (C1-C5). Expression level was normalized to β -actin (ACTB) and presented as mean and standard deviation (n \geq 3). Error bars represent standard deviations. (C) Immunohistochemical staining of *GOT2* in two tumors carrying the *GOT2* c.357A>T variant and in one control with WT-*GOT2*. Cytoplasmic aggregates were observed

only in *GOT2*-mutated tumors. **(D)** GOT2 activity measured in lymphoblastic *GOT2*-mutated (c.357A>T) and non-mutated cells (C1-C3).

Figure 4. **(A)** Succinate/fumarate ratios assessed by liquid chromatographic tandem-mass spectrometry (LC/MS) in 13 tumors assayed in the present study compared to SDH gene-mutated (n=9) and non-SDH gene-mutated controls (n=6). Tumor_1: tumor carrying the IDH1 and the c.223T>G *GOT2* variants; tumor_2: tumor carrying the c.357A>T *GOT2* variant; tumor_3: tumor carrying the OGDHL and PCK2 variants; tumor_4: tumor showing DNA methylation of SDHC. The black lines represent medians. **(B)** Hydroxyglutarate/isocitrate ratios assessed by LC/MS in nine tumors from the present study compared to SDH gene-mutated (n=9) and non-SDH gene-mutated controls (n=6). The IDH1-mutated tumor is indicated. The black lines represent medians. **(C)** α -Ketoglutarate/isocitrate ratios assessed by LC/MS in the *IDH3B*-mutated tumor compared to ten tumors from the present study, nine SDH gene-mutated cases and six non-SDH gene-mutated controls. The black lines represent medians. **(D)** Aspartate/glutamate ratios assessed by LC-MS in *GOT2* KD HeLa cells transfected with empty vector (EV), *GOT2* wild-type (WT) cDNA, and *GOT2*- c.357A>T cDNA. The ratios were reported as mean and standard deviation (n=3). Error bars represent standard deviations. A t-test was applied to test for differences between GOT WT and *GOT2*- c.357A>T transfected cells. **(E)** α -Ketoglutarate/citrate ratios assessed by LC-MS in *GOT2* KD HeLa cells transfected with EV, *GOT2* WT cDNA, and *GOT2*- c.357A>T cDNA. The ratios were reported as mean and standard deviation (n=3). Error bars represent standard deviations. A t-test was applied to test for differences between GOT WT and *GOT2*- c.357A>T transfected cells.

Figure 1

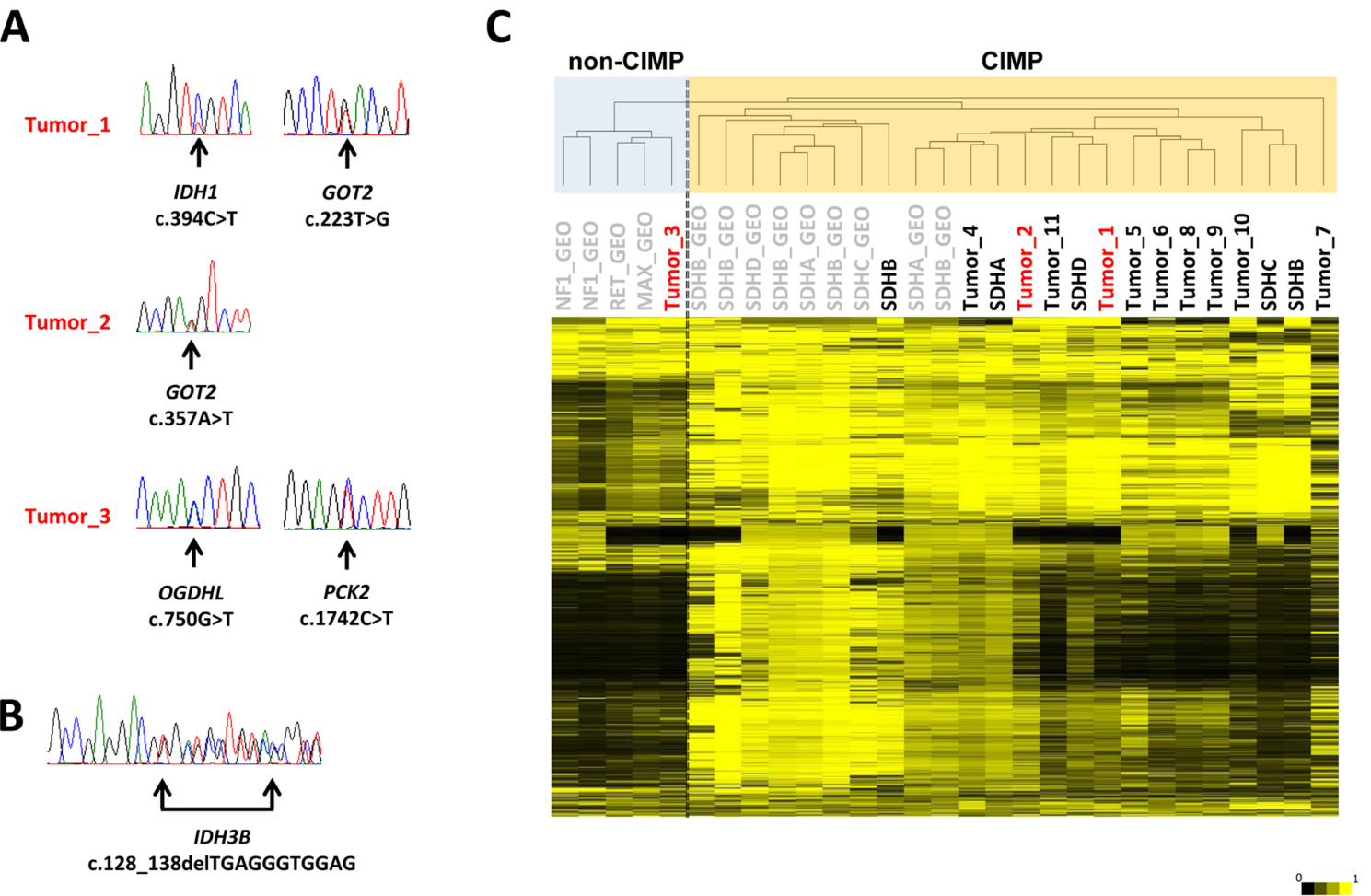
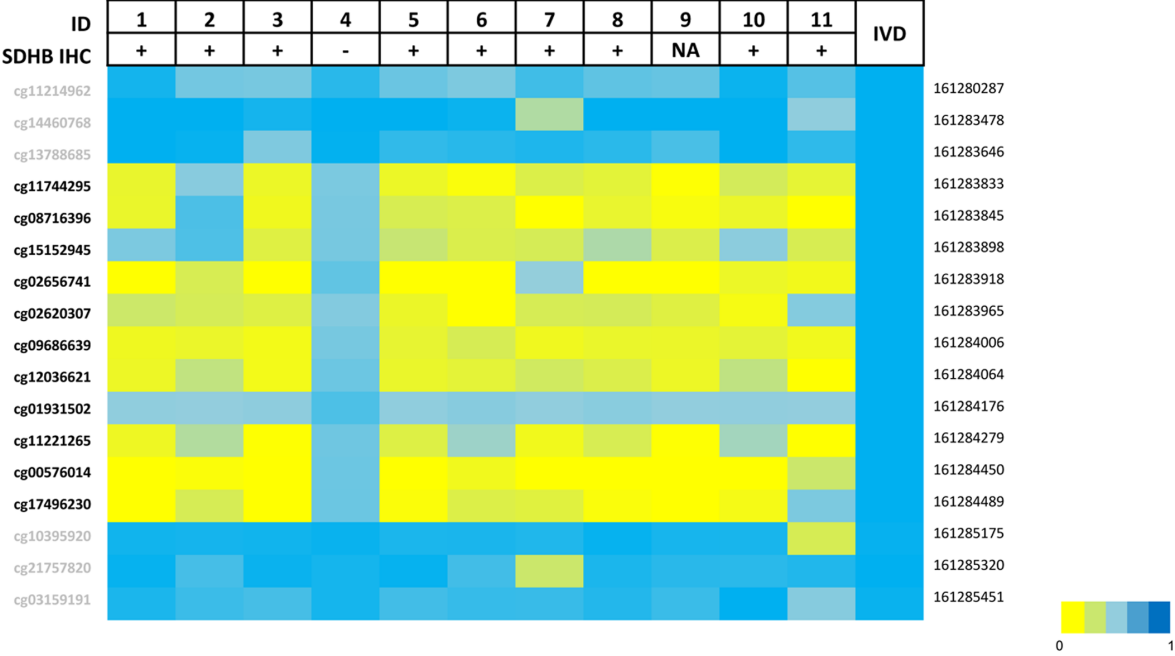


Figure 2

A



B

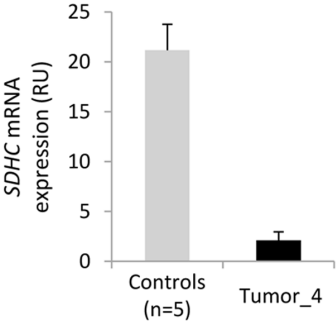


Figure 3

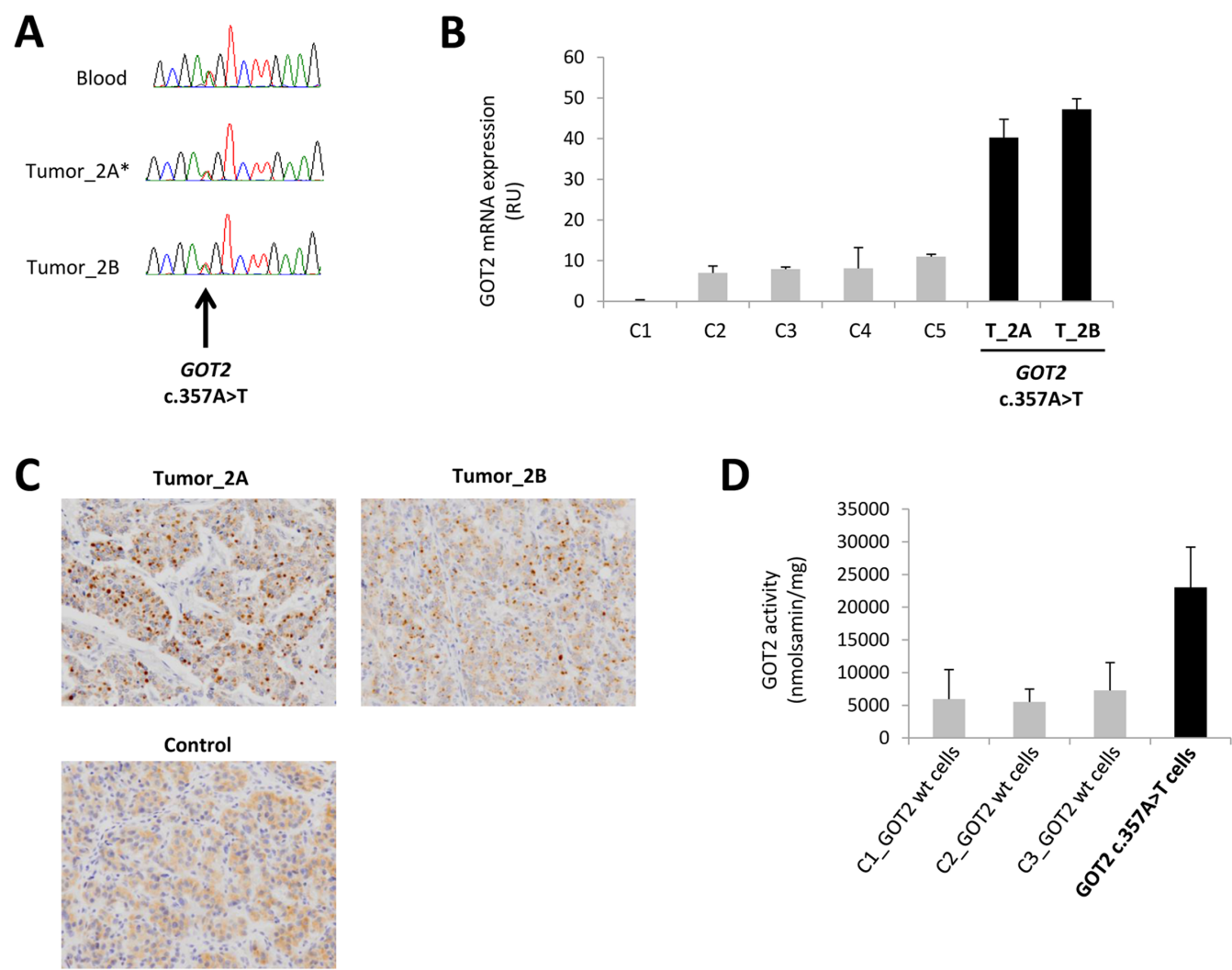


Figure 4

